fractal and fractional

Article

A Time Two-Mesh Finite Difference Numerical Scheme for the Symmetric Regularized Long Wave Equation

Jingying Gao *, Siriguleng He *, Qingmei Bai and Jie Liu

School of Mathematics and Big Data, Hohhot Minzu College, Hohhot 010051, China; baiqingmei@email.imnc.edu.cn (Q.B.); liujieem@email.imnc.edu.cn (J.L.)
* Correspondence: minzugjy@email.imnc.edu.cn (J.G.); t53000839@email.imnc.edu.cn (S.H.)

Abstract: The symmetric regularized long wave (SRLW) equation is a mathematical model used in many areas of physics; the solution of the SRLW equation can accurately describe the behavior of long waves in shallow water. To approximate the solutions of the equation, a time two-mesh (TT-M) decoupled finite difference numerical scheme is proposed in this paper to improve the efficiency of solving the SRLW equation. Based on the time two-mesh technique and two time-level finite difference method, the proposed scheme can calculate the velocity $u(x,t)$ and density $\rho(x,t)$ in the SRLW equation simultaneously. The linearization process involves a modification similar to the Gauss-Seidel method used for linear systems to improve the accuracy of the calculation to obtain solutions. By using the discrete energy and mathematical induction methods, the convergence results with $O(\tau_C^2+\tau_F+h^2)$ in the discrete L_∞-norm for $u(x,t)$ and in the discrete L_2-norm for $\rho(x,t)$ are proved, respectively. The stability of the scheme was also analyzed. Finally, some numerical examples, including error estimate, computational time and preservation of conservation laws, are given to verify the efficiency of the scheme. The numerical results show that the new method preserves conservation laws of four quantities successfully. Furthermore, by comparing with the original two-level nonlinear finite difference scheme, the proposed scheme can save the CPU time.

Keywords: SRLW equation; finite difference; time two-mesh; convergence analysis; conservation law

Citation: Gao, J.; He, S.; Bai, Q.; Liu, J. A Time Two-Mesh Finite Difference Numerical Scheme for the Symmetric Regularized Long Wave Equation. *Fractal Fract.* **2023**, *7*, 487. https://doi.org/10.3390/fractalfract7060487

Academic Editor: Carlo Cattani

Received: 23 May 2023
Revised: 16 June 2023
Accepted: 16 June 2023
Published: 19 June 2023

1. Introduction

The regularized long wave (RLW) equation [1,2] is a nonlinear partial differential equation that mainly describes the evolution of waves in shallow water channels and ion acoustics, etc. It is a simplified version of the more complex Korteweg-de Vries (KdV) equation [3], which includes higher-order nonlinearities and dispersion effects. The symmetric regularized long wave (SRLW) equation [4] is a modified version of the RLW equation that includes a symmetry-breaking term. This term allows for the formation of asymmetric solutions, making the SRLW equation a more realistic model for waves in shallow water channels.

In this paper, the following initial boundary value problem of the SRLW equation is considered:

$$\begin{cases} u_t+\rho_x+uu_x-u_{xxt}=0, \quad x_L\le x\le x_R, \ \ 0<t\le T, \\ \rho_t+u_x=0, \quad x_L\le x\le x_R, \ \ 0<t\le T, \\ u(x_L,t)=u(x_R,t)=0, \quad \rho(x_L,t)=\rho(x_R,t)=0, \quad 0<t\le T, \\ u(x,0)=u_0(x), \quad \rho(x,0)=\rho_0(x), \quad x_L\le x\le x_R, \end{cases} \tag{1}$$

where $u(x,t)$ and $\rho(x,t)$ are the fluid velocity and the density, respectively.

The SRLW equation has attracted significant attention and has been extensively studied in the literature. The existence of global attractors of the SRLW equation was studied in [5]. The travelling and solitary wave solutions of the SRLW equation were investigated by several methods including the exp-function method [6], the (G'/G)-expansion method [7,8], the tanh-function method [9,10], the Lie symmetry approach [11], the extended simple equation method [12], the analytical method [13], the tan $((\phi(\xi)/2))$-expansion method [14] and the sine–cosine method [15]. In [16,17], the spectral method and the Fourier pseudo-spectral method with a constraint operator were developed as approximations for the nonlinear term of the SRLW equation. Numerical solutions to the SRLW equation have also been studied by numerous methods, ranging from conservative finite difference schemes to mixed finite element methods. In their study, Wang et al. [18] introduced three conservative finite difference schemes that achieve second-order accuracy in both spatial and temporal domains. Their results indicate that each scheme is able to preserve energy conservation, but only the first scheme is capable of preserving mass conservation. Yimnet et al. [19] presented a novel finite difference method for the SRLW equation that utilizes a four-level average difference technique for solving the fluid velocity independently from the density. A coupled conservative three-level implicit scheme achieving fourth-order convergence rate was developed by Hu et al. [20]. Li [21] considered a weighted and compact conservative difference scheme that is decoupled and linearized in practical computation, thus requiring only the solution of two tridiagonal systems of linear algebraic equations at each time step. Bai et al. [22] investigated a two-layer conservative finite difference scheme for the SRLW equation with homogeneous boundary conditions and analyzed the scheme's convergence and stability using a discrete functional analysis method. Xu et al. [23] applied a mixed finite element method to solve the dissipative SRLW equations with damping term. He et al. [24] developed a fourth-order accurate compact difference scheme for the SRLW equation for a single nonlinear velocity form and conducted theoretical analysis using the discrete energy method.

In terms of numerical computation, the time two-mesh (TT-M) method, when combined with either the finite element method or the finite difference method, offers better computational efficiency in solving a broad range of nonlinear partial differential equations. For instance, Liu et al. [25] proposed the fast TT-M finite element method for solving the fractional water wave model and applied it successfully to other fractional models. Yin et al. [26] developed a TT-M finite element algorithm for solving a space fractional Allen-Cahn model and analyzed the problem of parameter selection in detail. The TT-M finite element method was also leveraged by Liu et al. [27] to numerically solve the 2D Gray-Scott model with space fractional derivatives. A nonlinear distributed order diffusion model was efficiently solved using the TT-M algorithm in conjunction with the H_1-Galerkin mixed finite element method by Wen et al. [28], both smooth and non-smooth solutions were considered. Additionally, Tian et al. [29] developed a finite element method equipped with the TT-M technique to solve the coupled Schrödinger-Boussinesq equations. Moreover, some studies have investigated combining the TT-M and finite difference methods to solve nonlinear fractional partial differential equations, such as the works of Qiu and Xu et al. [30,31], who proposed and analyzed a TT-M algorithm based on finite difference methods. The TT-M technique was also employed by Niu et al. [32] to develop a fast high-order compact difference scheme for the nonlinear distributed order fractional Sobolev model in porous media. Furthermore, He et al. [33] extended the application of the TT-M method by studying a primary scheme of second-order convergence in time and fourth-order in space for solving the nonlinear Schrödinger equation with a time two-mesh high-order compact difference scheme. Despite the extensive research on the TT-M method in various fields, to the best of our knowledge, no study on the application of the TT-M method combined with finite difference to the SRLW equation has been discovered. Hence, investigations on the TT-M finite difference method's performance when applied to the SRLW equation are still required.

The SRLW Equation (1) is a coupled system and most existing schemes found in the literature are also coupled and require nonlinear implementation, which results in prolonged CPU processing time. The objective of this paper is to develop a novel difference scheme that offers the following three main advantages for solving the SRLW equation:

(i) Based on the time two-mesh technique, we proposed a scheme that achieves decoupling and the nonlinear term of the system is linearized by using Taylor's formula for a function with three variables, which is different from the literature [32,33]. In [32,33], the time two-mesh scheme is formulated by using Taylor's formula for a function with one or two variables. As a result, our scheme becomes a linearized system in approximate numerical solution and can reduce the computational time. (ii) The scheme's convergence and stability have been verified through detailed proof, and the theoretical analysis process is more complex than that of existing methods, since the linearized scheme contains a function of three variables. (iii) The linearization process involves a modification similar to the Gauss-Seidel method used for linear systems to improve the accuracy of the calculation for solutions. The conservation law of four quantities is preserved in the new scheme at the discrete level.

The remaining part of this article is organized as follows. In Section 2, some notations and useful lemmas are given. In Section 3, the TT-M finite difference numerical scheme is presented. In Section 4, the convergence and stability of the scheme is analyzed. In Section 5, some numerical results are provided to test the theoretical results and computational efficiency of the scheme. Finally, in Section 6, we provide the conclusions of the paper.

2. Notations and Some Lemmas

As usual, the time interval $(0, T]$ and spatial interval $[x_L, x_R]$ are divided into N and J uniform partitions. The following notations will be used in this paper:

$$\left(u_j^n\right)_x = \frac{u_{j+1}^n - u_j^n}{h}, \quad \left(u_j^n\right)_{\bar{x}} = \frac{u_j^n - u_{j-1}^n}{h}, \quad \left(u_j^n\right)_{\hat{x}} = \frac{u_{j+1}^n - u_{j-1}^n}{2h},$$
$$\left(u_j^n\right)_t = \frac{u_j^{n+1} - u_j^n}{\tau}, \quad u_j^{n+\frac{1}{2}} = \frac{1}{2}(u_j^{n+1} + u_j^n), \quad \left(u_j^n\right)_{x\bar{x}} = \frac{u_{j+1}^n - 2u_j^n + u_{j-1}^n}{h^2},$$

where τ, h denote the uniform time and spatial step length, respectively, $x_j = x_L + jh$, $j = 0, 1, 2, \cdots, J$, $t_n = n\tau, n = 1, 2, \cdots, [T/\tau] = N$, superscript n denotes a quantity associated with the time level t_n, subscript j denotes a quantity associated with space mesh point x_j. In this paper, M denotes general constant, which may have a different value in a different place.

Since $u \to 0$ for $x \to +\infty$ or $x \to -\infty$, we may assume $u_{-1}^n = u_{J+1}^n = 0, 1 \le n \le N$ for simplicity, where $j = -1$ and $J + 1$ are ghost points. Let $H_{h,0}$ denote the set of mesh functions u^n defined on I_h with boundary conditions $u_{-1}^n = u_0^n = u_J^n = u_{J+1}^n = 0$. For any two mesh functions $u^n, w^n \in H_{h,0}$, we define the discrete inner product and norms as follows:

$$(u^n, w^n) = h\sum_{j=1}^{J-1} u_j^n w_j^n, \quad \|u^n\| = \sqrt{(u^n, u^n)}, \quad \|u^n\|_\infty = \max_{1\le j\le J-1} |u_j^n|.$$

Next, we present some useful lemmas.

Lemma 1 (See [24])**.** *For any mesh functions $u^n, w^n \in H_{h,0}$, we have*

$$(a)\ (u_x^n, w^n) = -(u^n, w_{\bar{x}}^n) = -(u^n, w_x^n), \quad (b)\ (u_{x\bar{x}}^n, w^n) = -(u_x^n, w_x^n), \quad (c)\ (u_{\hat{x}}^n, w^n) = -(u^n, w_{\hat{x}}^n).$$

Lemma 2 (See [33,34])**.** *Assume that a sequence of non-negative real numbers $\{a_j\}_{j=0}^\infty$ satisfying*

$$a_{n+1} \le \alpha + \beta \sum_{j=0}^{n} a_j \tau, \quad n \ge 0,$$

then there has the inequality $a_{n+1} \le (\alpha + \tau\beta a_0)e^{\beta(n+1)\tau}$, where $\alpha \ge 0, \beta$ and τ are positive constants.

Lemma 3 (See [22,34]). *For any discrete mesh function $u^n \in H_{h,0}$, there exists constants C_1 and C_2, such that*

$$\|u^n\|_\infty \le C_1\|u^n\| + C_2\|u_x^n\|.$$

3. The TT-M Finite Difference Scheme

In this paper, we studied a TT-M finite difference fast numerical method for the SRLW Equation (1). In order to give the TT-M finite difference scheme, firstly, the time interval $(0, T]$ is partitioned uniformly into P coarse time intervals and then each of them is divided into $s(2 \le s \in Z^+)$ fine time intervals. The coarse time mesh with the nodes $t_{ks} = k\tau_C(k = 1, \ldots, P)$ satisfying $0 = t_0 < t_s < t_{2s} < \cdots < t_{Ps} = T$ and the fine time mesh with the nodes $t_n = n\tau_F(n = 1, 2, \ldots, Ps = N)$ satisfying $0 = t_0 < t_1 < t_2 < \cdots < t_{Ps} = T$, where $\tau_C = s\tau_F$ and τ_F are the coarse time and the fine time step size, respectively.

Secondly, the truncation errors of the problem (1) are considered, let $v_j^n = u(x_j, t_n)$, $\varphi_j^n = \rho(x_j, t_n)$ be the exact solutions of $u(x, t)$ and $\rho(x, t)$ in term of the point (x_j, t_n), then we have

$$Er_j^n = (v_j^n)_t + (\varphi_j^{n+1})_{\hat{x}} - (v_j^n)_{x\bar{x}t} + \frac{1}{3}\left\{v_j^{n+\frac{1}{2}}(v_j^{n+\frac{1}{2}})_{\hat{x}} + \left[(v_j^{n+\frac{1}{2}})^2\right]_{\hat{x}}\right\}, \tag{2}$$

$$Es_j^n = (\varphi_j^n)_t + (v_j^n)_{\hat{x}}, \tag{3}$$

$$\begin{aligned} &v_0^n = v_J^n = 0, \varphi_0^n = \varphi_J^n = 0, \\ &v_j^0 = v_0(x_L + jh), \varphi_j^0 = \varphi_0(x_L + jh). \end{aligned}$$

By Taylor series expansion, we have

$$\begin{aligned} Er_j^n &= (u_t + \rho_x - u_{xxt} + uu_x)_{(x_j,t_n)} = O(h^2 + \tau), \\ Es_j^n &= (\rho_t + u_x)_{(x_j,t_n)} = O(h^2 + \tau). \end{aligned}$$

Next, based on Equations (2) and (3), a TT-M finite difference scheme for problem (1) is constructed with three steps.

Step 1: on the coarse time mesh, let $u_{C,j}^{ks} = u(x_j, t_{ks}), \rho_{C,j}^{ks} = \rho(x_j, t_{ks})$ be the numerical solutions of of $u(x, t)$ and $\rho(x, t)$ in term of the point (x_j, t_{ks}), then the coarse time nonlinear finite difference scheme is given as

$$(u_{C,j}^{ks})_t + (\rho_{C,j}^{(k+1)s})_{\hat{x}} - (u_{C,j}^{ks})_{x\bar{x}t} + \frac{1}{3}\left\{u_{C,j}^{ks+\frac{1}{2}}(u_{C,j}^{ks+\frac{1}{2}})_{\hat{x}} + \left[(u_{C,j}^{ks+\frac{1}{2}})^2\right]_{\hat{x}}\right\} = 0, \tag{4}$$

$$(\rho_{C,j}^{ks})_t + (u_{C,j}^{ks})_{\hat{x}} = 0, \tag{5}$$

$$\begin{aligned} &u_{C,0}^{ks} = u_{C,J}^{ks} = 0, \rho_{C,0}^{ks} = \rho_{C,J}^{ks} = 0, && k = 0, 1, \ldots, P, \\ &u_{C,j}^0 = u_0(x_L + jh), \rho_{C,j}^0 = \rho_0(x_L + jh), && j = 1, 2, \ldots, J - 1, \end{aligned}$$

where $u_{C,j}^{ks+\frac{1}{2}} = \frac{1}{2}(u_{C,j}^{(k+1)s} + u_{C,j}^{ks})$.

Step 2: based on the solutions u_C^{ks}, ρ_C^{ks} at time levels t_{ks} obtained from step 1, we apply the Lagrange's linear interpolation formula to compute $u_C^{ks-l}, \rho_C^{ks-l}$ at time levels $t_{ks-l}(l = 1, 2, \ldots, s - 1$ and $k = 1, 2, \ldots, P, ks - l = n)$, we have

$$u_C^{ks-l} = \frac{t_{ks-l} - t_{ks}}{t_{(k-1)s} - t_{ks}}u_C^{(k-1)s} + \frac{t_{ks-l} - t_{(k-1)s}}{t_{ks} - t_{(k-1)s}}u_C^{ks} = \frac{l}{s}u_C^{(k-1)s} + (1 - \frac{l}{s})u_C^{ks}, \tag{6}$$

$$\rho_C^{ks-l} = \frac{t_{ks-1} - t_{ks}}{t_{(k-1)s} - t_{ks}}\rho_C^{(k-1)s} + \frac{t_{ks-1} - t_{(k-1)s}}{t_{ks} - t_{(k-1)s}}\rho_C^{ks} = \frac{l}{s}\rho_C^{(k-1)s} + (1 - \frac{l}{s})\rho_C^{ks}. \tag{7}$$

Remark 1. *The Equation (7) is only employed for theoretical analysis of the scheme. In numerical simulation, the coarse numerical solutions ρ_C^{ks-l} are not needed for computation since they are not used in step 3.*

Step 3: based on all the coarse numerical solutions $u_{C,j}^n(n = 0,1,2,\ldots,Ps = N,$ $j = 1,2,\ldots,J-1)$ obtained in the first two steps, Taylor's formula is used to construct a linearized system on the fine time mesh, which is expressed as follows. Let $u_{F,j}^n = u(x_j,t_n), \rho_{F,j}^n = \rho(x_j,t_n)$ be the numerical solutions of $u(x,t)$ and $\rho(x,t)$ in term of the point (x_j,t_n) on the fine time mesh, then

$$\begin{aligned}(u_{F,j}^n)_t + (\rho_{F,j}^{n+1})_{\hat{x}} - (u_{F,j}^n)_{x\bar{x}t} + \frac{1}{6h}\Big[& f(u_{C,j-1}^{n+\frac{1}{2}}, u_{C,j}^{n+\frac{1}{2}}, u_{C,j+1}^{n+\frac{1}{2}}) \\ & + f_x(u_{C,j-1}^{n+\frac{1}{2}}, u_{C,j}^{n+\frac{1}{2}}, u_{C,j+1}^{n+\frac{1}{2}})(u_{F,j-1}^{n+\frac{1}{2}} - u_{C,j-1}^{n+\frac{1}{2}}) \\ & + f_y(u_{C,j+1}^{n+\frac{1}{2}}, u_{C,j}^{n+\frac{1}{2}}, u_{C,j+1}^{n+\frac{1}{2}})(u_{F,j}^{n+\frac{1}{2}} - u_{C,j}^{n+\frac{1}{2}}) \\ & + f_z(u_{C,j-1}^{n+\frac{1}{2}}, u_{C,j}^{n+\frac{1}{2}}, u_{C,j+1}^{n+\frac{1}{2}})(u_{F,j+1}^{n+\frac{1}{2}} - u_{C,j+1}^{n+\frac{1}{2}})\Big] = 0,\end{aligned} \tag{8}$$

$$(\rho_{F,j}^n)_t + (u_{F,j}^n)_{\hat{x}} = 0, \tag{9}$$

$$\begin{aligned}& u_{F,0}^n = u_{F,J}^n = 0, \quad \rho_{F,0}^n = \rho_{F,J}^n = 0, \\ & u_{F,j}^0 = u_0(x_L + jh), \quad \rho_{F,j}^0 = \rho_0(x_L + jh), \\ & j = 1,\ldots,J-1, \quad n = 0,1,2,\ldots,N,\end{aligned}$$

where $f(x,y,z) = (z-x)y + z^2 - x^2$ and

$$f_x(x,y,z) = -y - 2x, f_y(x,y,z) = z - x, f_z(x,y,z) = y + 2z$$

are the three partial derivatives of $f(x,y,z)$ with respect to x, y, z.

Remark 2. *Our method, similarly to the Gauss-Seidel method applied to linear systems, has been modified in order to enhance the accuracy of fine mesh solutions u_F^{n+1} by using u_F^n in calculation.*

4. Convergence Analysis and Stability of the TT-M Finite Difference Scheme

The focus of this section is on performing convergence analysis of the nonlinear system specifically on the coarse time mesh.

Theorem 1. *Suppose that the exact solutions v^n, φ^n to the initial boundary value problem Equation (1) is sufficiently smooth and let u_C^n, ρ_C^n be the numerical solutions on the coarse time mesh. Then,*

$$\|v^n - u_C^n\|_\infty \le O(h^2 + \tau_C), \|\varphi^n - \rho_C^n\| \le O(h^2 + \tau_C).$$

Proof. Denote $e_{C,j}^{ks} = v_j^{ks} - u_{C,j}^{ks}, \eta_{C,j}^{ks} = \varphi_j^{ks} - \rho_{C,j}^{ks}, 1 \le j \le J-1, 0 \le k \le P$. Subtracting Equation (4) from Equation (2) and Equation (5) from Equation (3), we obtain

$$\begin{aligned}Er_{C,j}^{ks} =& (e_{C,j}^{ks})_t + (\eta_{C,j}^{(k+1)s})_{\hat{x}} - (e_{C,j}^{ks})_{x\bar{x}t} \\ & + \frac{1}{3}\left\{ v_j^{ks+\frac{1}{2}}(v_j^{ks+\frac{1}{2}})_{\hat{x}} + \left[(v_j^{ks+\frac{1}{2}})^2\right]_{\hat{x}} \right\} - \frac{1}{3}\left\{ u_{C,j}^{ks+\frac{1}{2}}(u_{C,j}^{ks+\frac{1}{2}})_{\hat{x}} + \left[(u_{C,j}^{ks+\frac{1}{2}})^2\right]_{\hat{x}} \right\},\end{aligned} \tag{10}$$

$$Es_{C,j}^{ks} = (\eta_{C,j}^{ks})_t + (e_{C,j}^{ks})_{\hat{x}}. \tag{11}$$

The proof contains two cases. Firstly, we consider the case of $n = ks(k = 0, 1, 2, \ldots, P)$, then $n + 1 = (k + 1)s$. The initial and boundary condition satisfies

$$\begin{aligned} e^0_{C,j} = 0, \quad \eta^0_{C,j} = 0, \\ u^n_{C,0} = u^n_{C,J} = 0, \quad \rho^n_{C,0} = \rho^n_{C,J} = 0. \end{aligned}$$

Taking the inner product $(\cdot, \cdot)$ on both sides of Equation (10) with $e^{n+1}_C + e^n_C$, we have

$$\begin{aligned} (Er^n_C, e^{n+1}_C + e^n_C) &= ((e^{n+1}_C)_t, e^n_C + e^n_C) + ((\eta^{n+1}_C)_{\hat{x}}, e^{n+1}_C + e^n_C) \\ &- ((e^n_C)_{x\bar{x}t}, e^{ks+1}_C + e^n_C) + h \sum_{j=1}^{J-1} (\mathrm{I} + \mathrm{II})(e^{n+1}_{C,j} + e^n_{C,j}), \end{aligned} \tag{12}$$

where

$$\mathrm{I} = \frac{1}{3}\left[v^{n+\frac{1}{2}}_j (v^{n+\frac{1}{2}}_j)_{\hat{x}} - u^{n+\frac{1}{2}}_{C,j}(u^{n+\frac{1}{2}}_{C,j})_{\hat{x}}\right], \mathrm{II} = \frac{1}{3}\left\{\left[(v^{n+\frac{1}{2}}_j)^2\right]_{\hat{x}} - \left[(u^{n+\frac{1}{2}}_{C,j})^2\right]_{\hat{x}}\right\}.$$

Notice that

$$((e^n_C)_t, e^{n+1}_C + e^n_C) = \frac{1}{\tau_C}(\|e^{n+1}_C\|^2 - \|e^n_C\|^2), \tag{13}$$

$$((\eta^{n+1}_C)_{\hat{x}}, e^{n+1}_C + e^n_C) = -h \sum_{j=1}^{J-1}\left[\eta^{n+1}_{C,j}(e^{n+1}_{C,j} + e^n_{C,j})_{\hat{x}}\right], \tag{14}$$

$$-((e^n_C)_{x\bar{x}t}, e^{n+1}_C + e^n_C) = \frac{1}{\tau_C}(\|e^{n+1}_{C,x}\|^2 - \|e^n_{C,x}\|^2), \tag{15}$$

$$\begin{aligned} h \sum_{j=1}^{J-1} \mathrm{I} \cdot (e^{n+1}_{C,j} + e^n_{C,j}) = &- \frac{2}{3} h \sum_{j=1}^{J-1} (e^{n+\frac{1}{2}}_{C,j} \cdot v^{n+\frac{1}{2}}_j)_{\hat{x}} e^{n+\frac{1}{2}}_{C,j} \\ &- \frac{2}{3} h \sum_{j=1}^{J-1} (e^{n+\frac{1}{2}}_{C,j})_{\hat{x}} (e^{n+\frac{1}{2}}_{C,j+1} + e^{n+\frac{1}{2}}_{C,j-1}) u^{n+\frac{1}{2}}_{C,j}, \end{aligned} \tag{16}$$

$$\begin{aligned} h \sum_{j=1}^{J-1} \mathrm{II} \cdot (e^{n+1}_{C,j} + e^n_{C,j}) = &\frac{2}{3} h \sum_{j=1}^{J-1} (v^{n+\frac{1}{2}}_j \cdot e^{n+\frac{1}{2}}_{C,j})_{\hat{x}} e^{n+\frac{1}{2}}_{C,j} \\ &- \frac{2}{3} h \sum_{j=1}^{J-1} u^{n+\frac{1}{2}}_{C,j} e^{n+\frac{1}{2}}_{C,j} (e^{n+\frac{1}{2}}_{C,j})_{\hat{x}}, \end{aligned} \tag{17}$$

then substituting Equations (13)–(17) into (12), we have

$$\begin{aligned} \|e^{n+1}_C\|^2 + \|e^{n+1}_{C,x}\|^2 = &\|e^n_C\|^2 + \|e^n_{C,x}\|^2 + \tau_C h \sum_{j=1}^{J-1}\left[\eta^{n+1}_{C,j}(e^{n+1}_{C,j} + e^n_{C,j})_{\hat{x}}\right] \\ &+ \frac{2}{3}\tau_C h \sum_{j=1}^{J-1}\left[(e^{n+\frac{1}{2}}_{C,j})_{\hat{x}}(e^{n+\frac{1}{2}}_{C,j+1} + e^{n+\frac{1}{2}}_{C,j-1}) u^{n+\frac{1}{2}}_{C,j} + u^{n+\frac{1}{2}}_{C,j} e^{n+\frac{1}{2}}_{C,j}(e^{n+\frac{1}{2}}_{C,j})_{\hat{x}}\right] \\ &+ \tau_C(Er^n_C, e^{n+1}_C + e^n_C). \end{aligned} \tag{18}$$

From Cauchy–Schwarz inequality, we obtain

$$(Er^n_C, e^{n+1}_C + e^n_C) \le \|Er^n_C\|^2 + \frac{1}{2}(\|e^{n+1}_C\|^2 + \|e^n_C\|^2).$$

Using Lemma 1, the Equation (18) can be rewritten as

$$\begin{aligned}\|e_C^{n+1}\|^2 + \|e_{C,x}^{n+1}\|^2 \le \|e_C^n\|^2 + \|e_{C,x}^n\|^2 \\ + M\tau_C(\|\eta_C^{n+1}\|^2 + \|e_C^{n+1}\|^2 + \|e_C^n\|^2 + \|e_{C,x}^{n+1}\|^2 + \|e_{C,x}^n\|^2) + \tau_C\|Er_C^n\|^2.\end{aligned} \tag{19}$$

Similarly, taking the inner product $(\cdot, \cdot)$ on both sides of Equation (11) with $\eta_C^{n+1} + \eta_C^n$, we obtain

$$\|\eta_C^{n+1}\|^2 = \|\eta_C^n\|^2 - \tau_C h \sum_{j=1}^{J-1} (e_{C,j}^n)_{\hat{x}} (\eta_{C,j}^{n+1} + \eta_{C,j}^n) + \tau_C(Es_C^n, \eta_C^{n+1} + \eta_C^n). \tag{20}$$

From the Cauchy–Schwarz inequality, we have

$$(Es_C^n, \eta_C^{n+1} + \eta_C^n) \le \|Es_C^n\|^2 + \frac{1}{2}(\|\eta_C^{n+1}\|^2 + \|\eta_C^n\|^2).$$

Using Lemma 1, the Equation (20) can be rewritten as

$$\|\eta_C^{n+1}\|^2 \le \|\eta_C^n\|^2 + M\tau_C(\|e_{C,x}^n\|^2 + \|\eta_C^{n+1}\|^2 + \|\eta_C^n\|^2) + \tau_C\|Es_C^n\|^2. \tag{21}$$

Add Equations (19) and (21), we obtain

$$\begin{aligned}\|e_C^{n+1}\|^2 + \|e_{C,x}^{n+1}\|^2 + \|\eta_C^{n+1}\|^2 \le \|e_C^n\|^2 + \|e_{C,x}^n\|^2 + \|\eta_C^n\|^2 \\ + M\tau_C(\|\eta_C^{n+1}\|^2 + \|\eta_C^n\|^2 + \|e_C^{n+1}\|^2 + \|e_C^n\|^2 + \|e_{C,x}^{n+1}\|^2 + \|e_{C,x}^n\|^2) \\ + \tau_C\|Er_C^n\|^2 + \tau_C\|Es_C^n\|^2.\end{aligned} \tag{22}$$

Let $B_C^n = \|e_C^n\|^2 + \|e_{C,x}^n\|^2 + \|\eta_C^n\|^2$, then Equation (22) becomes

$$B_C^{n+1} - B_C^n \le M\tau_C(B_C^{n+1} + B_C^n) + M\tau_C(h^2 + \tau_C)^2,$$

and obtain

$$(1 - M\tau_C)(B_C^{n+1} - B_C^n) \le 2M\tau_C B_C^n + M\tau_C(h^2 + \tau_C)^2.$$

By taking τ_C small enough so that $(1 - M\tau_C) > \lambda > 0$, then

$$B_C^{n+1} - B_C^n \le M\tau_C B_C^n + M\tau_C(h^2 + \tau_C)^2. \tag{23}$$

Summing from 0 to $P - 1$ inequalities in Equation (23), we have

$$B_C^P - B_C^0 \le M\tau_C \sum_{n=1}^{P-1} B_C^n + M(h^2 + \tau_C)^2,$$

and using Lemma 2, we obtain

$$B_C^P \le [B_C^0 + M(h^2 + \tau_C)^2]e^{MP\tau_C}. \tag{24}$$

From Equation (24) and the initial and boundary condition, we have

$$\|e_C^n\| < O(h^2 + \tau_C), \|e_{C,x}^n\| < O(h^2 + \tau_C), \|\eta_C^n\| < O(h^2 + \tau_C). \tag{25}$$

Then using Lemma 3, we obtain

$$\|e_C^n\|_\infty < O(h^2 + \tau_C). \tag{26}$$

Secondly, we consider the case of $n = ks - l$, ($l = 1, 2, \ldots, s-1$ and $k = 1, 2, \ldots, P$, $ks - l = n$). Based on the Lagrange's interpolation formula, we obtain

$$\begin{aligned} v^{ks-l} &= \frac{t_{ks-l} - t_{ks}}{t_{(k-1)s} - t_{ks}} v^{(k-1)s} + \frac{t_{ks-l} - t_{(k-1)s}}{t_{ks} - t_{(k-1)s}} v^{ks} \\ &= \frac{l}{s} v^{(k-1)s} + (1 - \frac{l}{s}) v^{ks} + \frac{v''(\theta_1)}{2}(t - t_{(k-1)s})(t - t_{ks}), \quad \theta_1 \in (t_{(k-1)s}, t_{ks}), \end{aligned} \tag{27}$$

$$\begin{aligned} \varphi^{ks-l} &= \frac{t_{ks-l} - t_{ks}}{t_{(k-1)s} - t_{ks}} \varphi^{(k-1)s} + \frac{t_{ks-l} - t_{(k-1)s}}{t_{ks} - t_{(k-1)s}} \varphi^{ks} \\ &= \frac{l}{s} \varphi^{(k-1)s} + (1 - \frac{l}{s}) \varphi^{ks} + \frac{\varphi''(\theta_2)}{2}(t - t_{(k-1)s})(t - t_{ks}), \quad \theta_2 \in (t_{(k-1)s}, t_{ks}). \end{aligned} \tag{28}$$

Subtracting Equation (27) from (6), we have

$$\begin{aligned} v^{ks-l} - u_C^{ks-l} =& \frac{l}{s}(v^{(k-1)s} - u_C^{(k-1)s}) + (1 - \frac{l}{s})(v^{ks} - u_C^{ks}) \\ &+ \frac{v''(\theta_1)}{2}(t - t_{(k-1)s})(t - t_{ks}). \end{aligned}$$

Subtracting Equation (28) from (7), we obtain

$$\begin{aligned} \varphi^{ks-l} - \rho_C^{ks-l} =& \frac{l}{s}(\varphi^{(k-1)s} - \rho_C^{(k-1)s}) + (1 - \frac{l}{s})(\varphi^{ks} - \rho_C^{ks}) \\ &+ \frac{\varphi''(\theta_2)}{2}(t - t_{(k-1)s})(t - t_{ks}). \end{aligned}$$

Using (25), (26) and triangle inequality, we conclude

$$\|e_C^{ks-l}\|_\infty \le O(h^2 + \tau_C), \|\eta_C^{ks-l}\| \le O(h^2 + \tau_C).$$

We obtain the result of Theorem 1 by synthesizing the aforementioned two cases. □

Next, we give the convergence analysis of the scheme on the fine time mesh.

Theorem 2. *Suppose that the exact solutions v^n, φ^n to the initial boundary value problem Equation (1) is sufficiently smooth and let u_F^n, ρ_F^n be the numerical solutions on the fine time mesh. Then,*

$$\|v^n - u_F^n\|_\infty \le O(h^2 + \tau_C^2 + \tau_F), \|\varphi^n - \rho_F^n\| \le O(h^2 + \tau_C^2 + \tau_F).$$

Proof. Assume $e_{F,j}^n = v_j^n - u_{F,j}^n, \eta_{F,j}^n = \varphi_j^n - \rho_{F,j}^n, 1 \le j \le J-1, 0 \le n \le N$, Subtracting Equation (8) from Equation (2) and Equation (9) from Equation (3), we obtain

$$Er_{F,j}^n = (e_{F,j}^n)_t + (\eta_{F,j}^{n+1})_{\hat{x}} - (e_{F,j}^n)_{x\bar{x}t} + \frac{1}{6h}[(f_x e_{F,j-1}^{n+\frac{1}{2}} + f_y e_{F,j}^{n+\frac{1}{2}} + f_z e_{F,j+1}^{n+\frac{1}{2}}) + Q], \tag{29}$$

$$Es_{F,j}^n = (\eta_{F,j}^n)_t + (e_{F,j}^n)_{\hat{x}}, \tag{30}$$

where

$$\begin{aligned} Q =& \frac{1}{2}[(f_{xx}(e_{C,j-1}^{n+\frac{1}{2}})^2 + f_{yy}(e_{C,j}^{n+\frac{1}{2}})^2 + f_{zz}(e_{C,j+1}^{n+\frac{1}{2}})^2] \\ &+ [f_{xy} e_{C,j-1}^{n+\frac{1}{2}} e_{C,j}^{n+\frac{1}{2}} + f_{xz} e_{C,j-1}^{n+\frac{1}{2}} e_{C,j+1}^{n+\frac{1}{2}} + f_{yz} e_{C,j}^{n+\frac{1}{2}} e_{C,j+1}^{n+\frac{1}{2}}], \end{aligned}$$

and $f_{xx} = f_{xx}(\xi, \varepsilon, \delta)$, $f_{yy} = f_{yy}(\xi, \varepsilon, \delta)$, $f_{zz} = f_{zz}(\xi, \varepsilon, \delta)$, $f_{xy} = f_{xy}(\xi, \varepsilon, \delta)$, $f_{xz} = f_{xz}(\xi, \varepsilon, \delta)$, $f_{yz} = f_{yz}(\xi, \varepsilon, \delta)$ are the second order partial derivatives of $f(x, y, z)$, $\xi \in (v_{j-1}^n, u_{C,j-1}^n)$, $\varepsilon \in (v_j^n, u_{C,j}^n)$, $\delta \in (v_{j+1}^n, u_{C,j+1}^n)$.

Taking the inner product $(\cdot,\cdot)$ on both sides of Equation (29) with $e_F^{n+1}+e_F^n$, we have

$$\begin{aligned}&\|e_F^{n+1}\|^2+\|e_{F,x}^{n+1}\|^2=\|e_F^n\|^2+\|e_{F,x}^n\|^2+\tau_F h\sum_{j=1}^{J-1}\Big\{\eta_{F,j}^{n+1}\Big[(e_{F,j}^{n+1})_{\hat{x}}+(e_{F,j}^n)_{\hat{x}}\Big]\Big\}\\&-\frac{\tau_F}{3}\sum_{j=1}^{J-1}(f_x e_{F,j-1}^{n+\frac{1}{2}}+f_y e_{F,j}^{n+\frac{1}{2}}+f_z e_{F,j+1}^{n+\frac{1}{2}})e_{F,j}^{n+\frac{1}{2}}-\frac{\tau_F}{3}\sum_{j=1}^{J-1}Qe_{F,j}^{n+\frac{1}{2}}+2\tau_F(Er_F^n,e_F^{n+\frac{1}{2}}).\end{aligned}\tag{31}$$

Using $f_y=\frac{1}{2}(f_x+f_z)$ and $f_{xx}=-2, f_{yy}=0, f_{zz}=2, f_{xy}=-1, f_{xz}=0, f_{yz}=1$, we obtain

$$\begin{aligned}&\sum_{j=1}^{J-1}(f_x e_{F,j-1}^{n+\frac{1}{2}}+f_y e_{F,j}^{n+\frac{1}{2}}+f_z e_{F,j+1}^{n+\frac{1}{2}})e_{F,j}^{n+\frac{1}{2}}\\&=-(f_x e_{F,\bar{x}}^{n+\frac{1}{2}},e_F^{n+\frac{1}{2}})+\frac{3}{h}(f_y e_F^{n+\frac{1}{2}},e_F^{n+\frac{1}{2}})+(f_z e_{F,x}^{n+\frac{1}{2}},e_F^{n+\frac{1}{2}}),\end{aligned}\tag{32}$$

$$\begin{aligned}&\sum_{j=1}^{J-1}Qe_{F,j}^{n+\frac{1}{2}}=\frac{1}{2}\sum_{j=1}^{J-1}[f_{xx}(e_{C,j-1}^{n+\frac{1}{2}})^2+f_{yy}(e_{C,j}^{n+\frac{1}{2}})^2+f_{zz}(e_{C,j+1}^{n+\frac{1}{2}})^2]e_{F,j}^{n+\frac{1}{2}}\\&+\sum_{j=1}^{J-1}[f_{xy}e_{C,j-1}^{n+\frac{1}{2}}e_{C,j}^{n+\frac{1}{2}}+f_{xz}e_{C,j-1}^{n+\frac{1}{2}}e_{C,j+1}^{n+\frac{1}{2}}+f_{yz}e_{C,j}^{n+\frac{1}{2}}e_{C,j+1}^{n+\frac{1}{2}}]e_{F,j}^{n+\frac{1}{2}}\\&=((e_C^{n+\frac{1}{2}})_x^2,e_F^{n+\frac{1}{2}})-((e_C^{n+\frac{1}{2}})^2,e_{F,x}^{n+\frac{1}{2}})+(e_{C,x}^{n+\frac{1}{2}},e_C^{n+\frac{1}{2}}e_F^{n+\frac{1}{2}})-(e_C^{n+\frac{1}{2}},(e_C^{n+\frac{1}{2}}e_F^{n+\frac{1}{2}})_x).\end{aligned}\tag{33}$$

Using Lemma 1 and the Cauchy–Schwarz inequality, we have

$$\begin{aligned}&\frac{\tau_F}{3}(f_x e_{F,\bar{x}}^{n+\frac{1}{2}},e_F^{n+\frac{1}{2}})-\frac{\tau_F}{h}(f_y e_F^{n+\frac{1}{2}},e_F^{n+\frac{1}{2}})-\frac{\tau_F}{3}(f_z e_{F,x}^{n+\frac{1}{2}},e_F^{n+\frac{1}{2}})\\&\le M\tau_F(\|e_{F,x}^{n+\frac{1}{2}}\|^2+\|e_F^{n+\frac{1}{2}}\|^2),\end{aligned}\tag{34}$$

$$\begin{aligned}&-\frac{\tau_F}{3}((e_C^{n+\frac{1}{2}})_x^2,e_F^{n+\frac{1}{2}})+\frac{\tau_F}{3}((e_C^{n+\frac{1}{2}})^2,e_{F,x}^{n+\frac{1}{2}})\\&-\frac{\tau_F}{3}(e_{C,x}^{n+\frac{1}{2}},e_C^{n+\frac{1}{2}}e_F^{n+\frac{1}{2}})+\frac{\tau_F}{3}(e_C^{n+\frac{1}{2}},(e_C^{n+\frac{1}{2}}e_F^{n+\frac{1}{2}})_x)\\&\le M\tau_F(\|e_C^{n+\frac{1}{2}}\|_\infty^2\|e_C^{n+\frac{1}{2}}\|^2+\|e_C^{n+\frac{1}{2}}\|_\infty^2\|e_{C,x}^{n+\frac{1}{2}}\|^2+\|e_F^{n+\frac{1}{2}}\|^2+\|e_{F,x}^{n+\frac{1}{2}}\|^2),\end{aligned}\tag{35}$$

$$2\tau_F(Er_F^n,e_F^{n+\frac{1}{2}})\le\tau_F\|Er_F^n\|^2+M\tau_F\|e_F^{n+\frac{1}{2}}\|^2.\tag{36}$$

Substituting Equations (34) and (35) into (31), then

$$\begin{aligned}&\|e_F^{n+1}\|^2+\|e_{F,x}^{n+1}\|^2\\&\le\|e_F^n\|^2+\|e_{F,x}^n\|^2+M\tau_F(\|\eta_F^{n+1}\|^2+\|e_F^{n+1}\|^2+\|e_F^n\|^2+\|e_{F,x}^{n+1}\|^2+\|e_{F,x}^n\|^2)\\&+M\tau_F(\|e_C^{n+\frac{1}{2}}\|_\infty^2\|e_C^{n+\frac{1}{2}}\|^2+\|e_C^{n+\frac{1}{2}}\|_\infty^2\|e_{C,x}^{n+\frac{1}{2}}\|^2)+\tau_F\|Er_F^n\|^2.\end{aligned}\tag{37}$$

Taking the inner product $(\cdot,\cdot)$ on both sides of Equation (30) with $\eta_F^{n+1}+\eta_F^n$, we obtain

$$\|\eta_F^{n+1}\|^2\le\|\eta_F^n\|^2+M\tau_F(\|e_{F,x}^n\|^2+\|\eta_F^{n+1}\|^2+\|\eta_F^n\|^2)+\tau_F\|Es_F^n\|^2.\tag{38}$$

Add Equations (37) and (38), we have

$$\begin{aligned}
&\|e_F^{n+1}\|^2 + \|e_{F,x}^{n+1}\|^2 + \|\eta_F^{n+1}\|^2 \le \|e_F^n\|^2 + \|e_{F,x}^n\|^2 + \|\eta_F^n\|^2 \\
&+ M\tau_F(\|\eta_F^{n+1}\|^2 + \|\eta_F^n\|^2 + \|e_F^{n+1}\|^2 + \|e_F^n\|^2 + \|e_{F,x}^{n+1}\|^2 + \|e_{F,x}^n\|^2) \\
&+ M\tau_F(\|e_C^{n+\frac{1}{2}}\|_\infty^2 \|e_C^{n+\frac{1}{2}}\|^2 + \|e_C^{n+\frac{1}{2}}\|_\infty^2 \|e_{C,x}^{n+\frac{1}{2}}\|^2) \\
&+ \tau_F\|Er_F^n\|^2 + \tau_F\|Es_F^n\|^2.
\end{aligned} \tag{39}$$

Let $B_F^n = \|e_F^n\|^2 + \|e_{F,x}^n\|^2 + \|\eta_F^n\|^2$, then

$$\begin{aligned}
B_F^{n+1} - B_F^n \le M\tau_F(B_F^{n+1} + B_F^n) + M\tau_F(\|e_C^{n+\frac{1}{2}}\|_\infty^2 \|e_C^{n+\frac{1}{2}}\|^2 + \|e_C^{n+\frac{1}{2}}\|_\infty^2 \|e_{C,x}^{n+\frac{1}{2}}\|^2) \\
+\tau_F\|Er_F^n\|^2 + \tau_F\|Es_F^n\|^2,
\end{aligned}$$

and obtain

$$(1 - M\tau_F)(B_F^{n+1} - B_F^n) \le 2M\tau_F B_F^n + M\tau_F(h^4 + \tau_C^4 + \tau_F^2).$$

By taking τ_F small enough so that $(1 - M\tau_F) > \lambda > 0$, then

$$B_F^{n+1} - B_F^n \le M\tau_F(h^4 + \tau_C^4 + \tau_F^2) + M\tau_F B_F^n. \tag{40}$$

Summing from 0 to $N-1$ inequalities in Equation (40), we obtain

$$B_F^N \le B_F^0 + M(h^4 + \tau_C^4 + \tau_F^2) + M\tau_F \sum_{n=0}^{N-1} B_F^n. \tag{41}$$

Using Lemma 2, we obtain

$$B_F^N \le [B_F^0 + M(h^4 + \tau_C^4 + \tau_F^2)]e^{MN\tau_F}. \tag{42}$$

From Equation (42) and the initial and boundary condition, we have

$$\|e_F^n\| \le O(h^2 + \tau_C^2 + \tau_F), \|e_{F,x}^n\| \le O(h^2 + \tau_C^2 + \tau_F), \|\eta_F^n\| < O(h^2 + \tau_C^2 + \tau_F). \tag{43}$$

Using Lemma 3, it led to

$$\|e_F^n\|_\infty \le O(h^2 + \tau_C^2 + \tau_F). \tag{44}$$

This completes the proof of Theorem 2. □

Next, we prove stability of the scheme on the coarse time mesh.

Theorem 3. *Suppose that $u_0 \in H_{h,0}[x_L, x_R]$, if τ_C and h are sufficiently small, then the proposed scheme (4)–(5) is stable with respect to the initial conditions.*

Proof. The proof contains two cases. Firstly, we consider the case of $n = ks(k = 0, 1, 2, \ldots, P)$. Taking the inner product $(\cdot, \cdot)$ on both sides of Equation (4) with $u_C^{n+1} + u_C^n$, we have

$$\begin{aligned}
&\left\|u_C^{n+1}\right\|^2 - \|u_C^n\|^2 + \left\|u_{C,x}^{n+1}\right\|^2 - \|u_{C,x}^n\|^2 \\
&+ \tau_C h \sum_{j=1}^{J-1} [-\rho_{C,j}^{n+1}(u_{C,j}^{n+1})_{\hat{x}} - \rho_{C,j}^{n+1}(u_{C,j}^n)_{\hat{x}}] = 0.
\end{aligned} \tag{45}$$

Taking the inner product $(\cdot, \cdot)$ on both sides of Equation (5) with $\rho_C^{n+1} + \rho_C^n$, we obtain

$$\|\rho_C^{n+1}\|^2 - |\rho_C^n\|^2 + \tau_C h \sum_{j=1}^{J-1} [(u_{C,j}^n)_{\hat{x}}\rho_{C,j}^{n+1} + (u_{C,j}^n)_{\hat{x}}\rho_{C,j}^n] = 0. \tag{46}$$

Add Equations (45) and (46), we obtain

$$\begin{aligned}
&\|u_C^{n+1}\|^2+\|u_{C,x}^{n+1}\|^2+\|\rho_C^{n+1}\|^2=\|u_C^n\|^2+\|u_{C,x}^n\|^2+\|\rho_C^n\|^2\\
&\quad+\tau_C h\sum_{j=1}^{J-1}\rho_{C,j}^{n+1}(u_{C,j}^{n+1})_{\hat{x}}-\tau_C h\sum_{j=1}^{J-1}(u_{C,j}^n)_{\hat{x}}\rho_{C,j}^n\\
&\le\|u_C^n\|^2+\|u_{C,x}^n\|^2+|\rho_C^n\|^2\\
&\quad+M\tau_C(\|\rho_C^{n+1}\|^2+\|\rho_C^n\|^2+\|u_C^{n+1}\|^2+\|u_C^n\|^2+\|u_{C,x}^{n+1}\|^2+\|u_{C,x}^n\|^2).
\end{aligned} \tag{47}$$

Let $D_C^n=\|u_C^n\|^2+\|u_{C,x}^n\|^2+\|\rho_C^n\|^2$, then Equation (47) becomes

$$D_C^{n+1}-D_C^n\le M\tau_C(D_C^{n+1}+D_C^n),$$

and obtain

$$(1-M\tau_C)(D_C^{n+1}-D_C^n)\le 2M\tau_C D_C^n.$$

By taking τ_C small enough so that $1-M\tau_C>\lambda>0$, then

$$D_C^{n+1}-D_C^n\le M\tau_C D_C^n. \tag{48}$$

Summing from 0 to $P-1$ inequalities in Equation (48), we have

$$D_C^N\le D_C^0+M\tau_C\sum_{n=0}^{N-1}D_C^n,$$

and using Lemma 2, we obtain

$$D_C^N\le D_C^0e^{MT}, \tag{49}$$

that is

$$\|u_C^n\|^2+\|u_{C,x}^n\|^2+\|\rho_C^n\|^2\le M(\|u_C^0\|^2+\|u_{C,x}^0\|^2+\|\rho_C^0\|^2).$$

Secondly, we consider the case of $n=ks-l$, $(l=1,2,\dots,s-1$ and $k=1,2,\dots,P, ks-l=n)$. From Equations (6) and (7), we obtain

$$\begin{aligned}
\|u_C^{ks-l}\|&\le\frac{l}{s}\|u_C^{(k-1)s}\|+(1-\frac{l}{s})\|u_C^{ks}\|\le M(\|u_C^0\|+\|u_{C,x}^0\|+\|\rho_C^0\|),\\
\|\rho_C^{ks-l}\|&\le\frac{l}{s}\|\rho_C^{(k-1)s}\|+(1-\frac{l}{s})\|\rho_C^{ks}\|\le M(\|u_C^0\|+\|u_{C,x}^0\|+\|\rho_C^0\|).
\end{aligned}$$

The results obtained in the aforementioned two cases mean that the solution of scheme (4)–(5) is stable on the coarse time mesh. This completes the proof of Theorem 3. □

Next, we present stability analysis of the scheme on the fine time mesh.

Theorem 4. *Suppose that $u_0\in H_{h,0}[x_L,x_R]$, if τ_F and h are sufficiently small, then the proposed scheme (8)–(9) is stable with respect to the initial conditions.*

Proof. Taking the inner product $(\cdot,\cdot)$ on both sides of Equation (8) with $u_F^{n+1}+u_F^n$, we have

$$\begin{aligned}\frac{1}{\tau_F}(\|u_F^{n+1}\|^2+\|u_{F,x}^{n+1}\|^2)&=\frac{1}{\tau_F}(\|u_F^n\|^2+\|u_{F,x}^n\|^2)\\&-h\sum_{j=1}^{J-1}[-\rho_{F,j}^{n+1}(u_{F,j}^{n+1})_{\hat{x}}-\rho_{F,j}^{n+1}(u_{F,j}^n)_{\hat{x}}]\\&-\frac{1}{3}\sum_{j=1}^{J-1}[(u_{C,j+1}^{n+\frac{1}{2}}-u_{C,j-1}^{n+\frac{1}{2}})u_{C,j}^{n+\frac{1}{2}}+(u_{C,j+1}^{n+\frac{1}{2}})^2-(u_{C,j-1}^{n+\frac{1}{2}})^2]u_{F,j}^{n+\frac{1}{2}}\\&-\frac{1}{3}\sum_{j=1}^{J-1}(f_xu_{F,j-1}^{n+\frac{1}{2}}+f_yu_{F,j}^{n+\frac{1}{2}}+f_zu_{F,j+1}^{n+\frac{1}{2}})u_{F,j}^{n+\frac{1}{2}}\\&+\frac{1}{3}\sum_{j=1}^{J-1}(f_xu_{C,j-1}^{n+\frac{1}{2}}+f_yu_{C,j}^{n+\frac{1}{2}}+f_zu_{C,j+1}^{n+\frac{1}{2}})u_{F,j}^{n+\frac{1}{2}}.\end{aligned}\tag{50}$$

From the Cauchy–Schwarz inequality, we obtain

$$\begin{aligned}&-\frac{1}{3}\sum_{j=1}^{J-1}[(u_{C,j+1}^{n+\frac{1}{2}}-u_{C,j-1}^{n+\frac{1}{2}})u_{C,j}^{n+\frac{1}{2}}+(u_{C,j+1}^{n+\frac{1}{2}})^2-(u_{C,j-1}^{n+\frac{1}{2}})^2]u_{F,j}^{n+\frac{1}{2}}\\&\le M(\|u_C^{n+\frac{1}{2}}\|_\infty^2\|u_C^{n+\frac{1}{2}}\|^2+\|u_C^{n+\frac{1}{2}}\|_\infty^2\|u_{C,x}^{n+\frac{1}{2}}\|^2+\|u_F^{n+\frac{1}{2}}\|^2+\|u_{F,x}^{n+\frac{1}{2}}\|^2),\end{aligned}\tag{51}$$

$$-\frac{1}{3}\sum_{j=1}^{J-1}(f_xu_{F,j-1}^{n+\frac{1}{2}}+f_yu_{F,j}^{n+\frac{1}{2}}+f_zu_{F,j+1}^{n+\frac{1}{2}})u_{F,j}^{n+\frac{1}{2}}\le M(\|u_F^{n+\frac{1}{2}}\|^2+\|u_{F,x}^{n+\frac{1}{2}}\|^2),\tag{52}$$

$$\begin{aligned}&\frac{1}{3}\sum_{j=1}^{J-1}(f_xu_{C,j-1}^{n+\frac{1}{2}}+f_yu_{C,j}^{n+\frac{1}{2}}+f_zu_{C,j+1}^{n+\frac{1}{2}})u_{F,j}^{n+\frac{1}{2}}\\&\le M(\|u_C^{n+\frac{1}{2}}\|^2+\|u_{C,x}^{n+\frac{1}{2}}\|^2+\|u_F^{n+\frac{1}{2}}\|^2+\|u_{F,x}^{n+\frac{1}{2}}\|^2),\end{aligned}\tag{53}$$

then substituting Equations (51)–(53) into (50), we have

$$\begin{aligned}&\|u_F^{n+1}\|^2+\|u_{F,x}^{n+1}\|^2\le\|u_F^n\|^2+\|u_{F,x}^n\|^2+\tau_Fh\sum_{j=1}^{J-1}[\rho_{F,j}^{n+1}(u_{F,j}^{n+1})_{\hat{x}}+\rho_{F,j}^{n+1}(u_{F,j}^n)_{\hat{x}}]\\&+M\tau_F(\|u_C^{n+\frac{1}{2}}\|_\infty^2\|u_C^{n+\frac{1}{2}}\|^2+\|u_C^{n+\frac{1}{2}}\|_\infty^2\|u_{C,x}^{n+\frac{1}{2}}\|^2+\|u_C^{n+\frac{1}{2}}\|^2+\|u_{C,x}^{n+\frac{1}{2}}\|^2)\\&+M\tau_F(\|u_F^{n+\frac{1}{2}}\|^2+\|u_{F,x}^{n+\frac{1}{2}}\|^2).\end{aligned}\tag{54}$$

Taking the inner product $(\cdot,\cdot)$ on both sides of Equation (9) with $\rho_F^{n+1}+\rho_F^n$, we obtain

$$\|\rho_F^{n+1}\|^2=\|\rho_F^n\|^2-\tau_Fh\sum_{j=1}^{J-1}[(u_{F,j}^n)_{\hat{x}}\rho_{F,j}^{n+1}+(u_{F,j}^n)_{\hat{x}}\rho_{F,j}^n].\tag{55}$$

Add Equations (54) and (55), we obtain

$$\begin{aligned}\|u_F^{n+1}\|^2+\|u_{F,x}^{n+1}\|^2+\|\rho_F^{n+1}\|^2&\le\|u_F^n\|^2+\|u_{F,x}^n\|^2+\|\rho_F^n\|^2\\&+M\tau_F(\|u_F^{n+1}\|^2+\|u_{F,x}^n\|^2+\|u_{F,x}^{n+1}\|^2+\|u_{F,x}^n\|^2+\|\rho_F^{n+1}\|^2+\|\rho_F^n\|^2)\\&+M\tau_F(\|u_C^{n+\frac{1}{2}}\|_\infty^2\|u_C^{n+\frac{1}{2}}\|^2+\|u_C^{n+\frac{1}{2}}\|_\infty^2\|u_{C,x}^{n+\frac{1}{2}}\|^2+\|u_C^{n+\frac{1}{2}}\|^2+\|u_{C,x}^{n+\frac{1}{2}}\|^2).\end{aligned}\tag{56}$$

Let $D_F^n = \|u_F^n\|^2 + \|u_{F,x}^n\|^2 + \|\rho_F^n\|^2$, then combine with the result of Theorem 3, the Equation (56) becomes

$$D_F^{n+1} - D_F^n \leq M\tau_F(D_F^{n+1} + D_F^n) + M\tau_F(\|u_C^0\|^2 + \|u_{C,x}^0\|^2),$$

and obtain

$$(1 - M\tau_F)(D_F^{n+1} - D_F^n) \leq 2M\tau_F D_F^n + M\tau_F(\|u_C^0\|^2 + \|u_{C,x}^0\|^2).$$

By taking τ_F small enough so that $1 - M\tau_F > \lambda > 0$, then

$$D_F^{n+1} - D_F^n \leq M\tau_F D_F^n + M\tau_F(\|u_C^0\|^2 + \|u_{C,x}^0\|^2). \tag{57}$$

Summing from 0 to $N-1$ inequalities in Equation (57), we obtain

$$\sum_{n=0}^{N-1}(D_F^{n+1} - D_F^n) \leq M\tau_F \sum_{n=0}^{N-1} D_F^n + M(\|u_C^0\|^2 + \|u_{C,x}^0\|^2), \tag{58}$$

and then

$$D_F^N \leq D_F^0 + M\tau_F \sum_{n=0}^{N-1} D_F^n + M(\|u_C^0\|^2 + \|u_{C,x}^0\|^2). \tag{59}$$

Using Lemma 2, we obtain

$$D_F^N \leq [D_F^0 + M\|u_C^0\|^2 + \|u_{C,x}^0\|^2)]e^{MT}, \tag{60}$$

that is

$$\|u_F^n\|^2 + \|u_{F,x}^n\|^2 + \|\rho_F^n\|^2 \leq M(\|u_F^0\|^2 + \|u_{F,x}^0\|^2 + \|\rho_F^0\|^2 + \|u_C^0\|^2 + \|u_{C,x}^0\|^2). \tag{61}$$

Notice that $\|u_C^0\|^2 = \|u_F^0\|^2$, $\|u_{C,x}^0\|^2 = \|u_{F,x}^0\|^2$, then

$$\|u_F^n\|^2 + \|u_{F,x}^n\|^2 + \|\rho_F^n\|^2 \leq M(\|u_F^0\|^2 + \|u_{F,x}^0\|^2 + \|\rho_F^0\|^2), \tag{62}$$

which indicates that the solution of scheme (8)–(9) is stable on the fine time mesh. This completes the proof of Theorem 4. □

5. Numerical Results

This section provides some numerical examples aimed at demonstrating the accuracy and computational time of the TT-M finite difference scheme that was discussed in Section 3. All simulations were implemented using a Intel(R) i7-10710U 1.61 GHz CPU and 16 GB memory personal computer running Windows 10 and Matlab R2019b. The SRLW equation is represented in the following formation:

$$\begin{array}{ll} u_t + \rho_x + uu_x - u_{xxt} = 0, & -40 \leq x \leq 40,\ \ 0 < t \leq 4, \\ \rho_t + u_x = 0, & -40 \leq x \leq 40,\ \ 0 < t \leq 4, \\ u(x_L, t) = u(x_R, t) = 0,\ \ \rho(x_L, t) = \rho(x_R, t) = 0, & 0 < t \leq 4, \\ u(x, 0) = u_0(x),\ \ \rho(x, 0) = \rho_0(x), & -40 \leq x \leq 40. \end{array}$$

and consider the following initial conditions

$$u_0(x) = \frac{5}{2}\operatorname{sech}^2\frac{\sqrt{5}}{6}x, \quad \rho_0(x) = \frac{5}{3}\operatorname{sech}^2\frac{\sqrt{5}}{6}x.$$

The exact solitary wave solution [4] of the SRLW Equation (1) has the following form

$$u(x,t) = \frac{3(v^2-1)}{v}\operatorname{sech}^2\left(\sqrt{\frac{v^2-1}{4v^2}}(x-vt)\right),$$
$$\rho(x,t) = \frac{3(v^2-1)}{v^2}\operatorname{sech}^2\left(\sqrt{\frac{v^2-1}{4v^2}}(x-vt)\right),$$

which takes the form of

$$u(x,t) = \frac{5}{2}\operatorname{sech}^2\frac{\sqrt{5}}{6}\left(x-\frac{3}{2}t\right), \quad \rho(x,t) = \frac{5}{3}\operatorname{sech}^2\frac{\sqrt{5}}{6}\left(x-\frac{3}{2}t\right),$$

when we set $v = 1.5$.

Next, we presented some values of error, convergence rate, conservation laws and long time simulation of the proposed scheme.

5.1. Error and Convergence Rate

We define the error and convergence rate by the following formula:

$$e_m(h,\tau) = \|v^n - u_m^n\|_\infty, \;\; \eta_m(h,\tau) = \|\varphi^n - \rho_m^n\|,$$
$$uRate_m^x = \log_2\left(\frac{e_m(2h,4\tau)}{e_m(h,\tau)}\right), \; \rho Rate_m^x = \log_2\left(\frac{\eta_m(2h,4\tau)}{\eta_m(h,\tau)}\right),$$
$$uRate_m^t = \log_2\left(\frac{e_m(2h,2\tau)}{e_m(h,\tau)}\right), \; \rho Rate_m^t = \log_2\left(\frac{\eta_m(2h,2\tau)}{\eta_m(h,\tau)}\right),$$

where m represents the TT-M finite difference scheme or the standard nonlinear finite difference (SNFD) scheme in [22]. We set $\tau_C = 4\tau_F$ in the whole numerical illustration process.

In order to illustrate the advantage of this approach, we calculated the error, convergence rate and computational time of the presented scheme and compared these numerical results with those obtained from scheme in [22]. Tables 1 and 2 present discrete norm errors, the corresponding convergence rates and the time cost for both the TT-M finite difference scheme and the SNFD scheme in [22] under $\tau_F = h^2$ and $h = \tau_F$, respectively. We recorded the error of both schemes at the final time $t = 4$ for various mesh steps. The results from the new scheme show nearly identical important values as those obtained by the SNFD scheme in [22]. In term of the convergence rate, the results indicate that both the TT-M finite difference scheme and the SNFD scheme achieve approximately second-order convergence in space when $\tau_F = h^2$ and first-order in time when $h = \tau_F$, which confirming the theoretical results in Theorem 2. Especially, the proposed scheme achieves a remarkable reduction in computation time of over 30 percent as compared to the SNFD scheme under $\tau_F = h^2$ and nearly half the computational time of the SNFD scheme under $h = \tau_F$. The obtained results demonstrate a clear improvement achieved by our scheme over the previous method reported by [22].

The 3D images of numerical solutions of $u(x,t)$ and $\rho(x,t)$ computed by the present scheme were shown in Figure 1. From the graph, one can see the propagation state of waves over a period of time. Figure 2 illustrates the exact and numerical solutions of $u(x,t)$ and $\rho(x,t)$ at $t = 4$ obtained by the present scheme. It is evident that our numerical solutions exhibit an excellent correspondence with the exact solution. Furthermore, the CPU times of the two schemes are plotted in Figure 3 under $\tau_F = h^2$ and $h = \tau_F$, respectively. From the figure, it is also can be seen that the present scheme can significantly decrease computation time. To sum up, compared with the method in [22], the scheme proposed in this paper not only ensures error and convergence order, but also greatly reduces computational time.

Table 1. The errors and convergence rates with $\tau_F = h^2$.

SNFD Scheme in [22]					
(h, τ_F)	$e_{SNFD}(h, \tau_F)$	$uRate^x_{SNFD}$	$\eta_{SNFD}(h, \tau_F)$	$\rho Rate^x_{SNFD}$	**CPU(s)**
$\left(\frac{1}{2}, \frac{1}{4}\right)$	8.2798×10^{-2}	—	2.9797×10^{-1}	—	0.14
$\left(\frac{1}{4}, \frac{1}{16}\right)$	2.0361×10^{-2}	2.02	7.3503×10^{-2}	2.02	0.51
$\left(\frac{1}{8}, \frac{1}{64}\right)$	5.0629×10^{-3}	2.01	1.8306×10^{-2}	2.01	12.30
$\left(\frac{1}{16}, \frac{1}{256}\right)$	1.2641×10^{-3}	2.00	4.5719×10^{-3}	2.00	136.31
$\left(\frac{1}{32}, \frac{1}{1024}\right)$	3.1597×10^{-4}	2.00	1.1427×10^{-3}	2.00	1943.47
Present scheme					
(h, τ_F)	$e_{TT-M}(h, \tau_F)$	$uRate^x_{TT-M}$	$\eta_{TT-M}(h, \tau_F)$	$\rho Rate^x_{TT-M}$	**CPU(s)**
$\left(\frac{1}{2}, \frac{1}{4}\right)$	8.3934×10^{-2}	—	3.0015×10^{-1}	—	0.10
$\left(\frac{1}{4}, \frac{1}{16}\right)$	2.0360×10^{-2}	2.04	7.3555×10^{-2}	2.03	0.30
$\left(\frac{1}{8}, \frac{1}{64}\right)$	5.0616×10^{-3}	2.01	1.8308×10^{-2}	2.01	7.53
$\left(\frac{1}{16}, \frac{1}{256}\right)$	1.2639×10^{-3}	2.00	4.5721×10^{-3}	2.00	76.99
$\left(\frac{1}{32}, \frac{1}{1024}\right)$	3.1596×10^{-4}	2.00	1.1427×10^{-3}	2.00	1297.88

Table 2. The errors and convergence rates with $h = \tau_F$.

SNFD Scheme in [22]					
(h, τ_F)	$e_{SNFD}(h, \tau_F)$	$uRate^t_{SNFD}$	$\eta_{SNFD}(h, \tau_F)$	$\rho Rate^t_{SNFD}$	**CPU(s)**
$\left(\frac{1}{8}, \frac{1}{8}\right)$	3.1920×10^{-2}	—	1.1381×10^{-1}	—	2.47
$\left(\frac{1}{16}, \frac{1}{16}\right)$	1.5552×10^{-2}	1.04	5.5256×10^{-2}	1.04	14.09
$\left(\frac{1}{32}, \frac{1}{32}\right)$	7.6748×10^{-3}	1.02	2.7221×10^{-2}	1.02	109.20
$\left(\frac{1}{64}, \frac{1}{64}\right)$	3.8121×10^{-3}	1.01	1.3509×10^{-2}	1.01	770.01
$\left(\frac{1}{128}, \frac{1}{128}\right)$	1.8997×10^{-3}	1.00	6.7298×10^{-3}	1.00	5792.53
Present scheme					
(h, τ_F)	$e_{TT-M}(h, \tau_F)$	$uRate^t_{TT-M}$	$\eta_{TT-M}(h, \tau_F)$	$\rho Rate^t_{TT-M}$	**CPU(s)**
$\left(\frac{1}{8}, \frac{1}{8}\right)$	3.1962×10^{-2}	—	1.1414×10^{-1}	—	1.49
$\left(\frac{1}{16}, \frac{1}{16}\right)$	1.5540×10^{-2}	1.04	5.5323×10^{-2}	1.04	7.10
$\left(\frac{1}{32}, \frac{1}{32}\right)$	7.6694×10^{-3}	1.02	2.7237×10^{-2}	1.02	51.40
$\left(\frac{1}{64}, \frac{1}{64}\right)$	3.8102×10^{-3}	1.01	1.3513×10^{-2}	1.01	414.33
$\left(\frac{1}{128}, \frac{1}{128}\right)$	1.8991×10^{-3}	1.00	6.7308×10^{-3}	1.01	3289.71

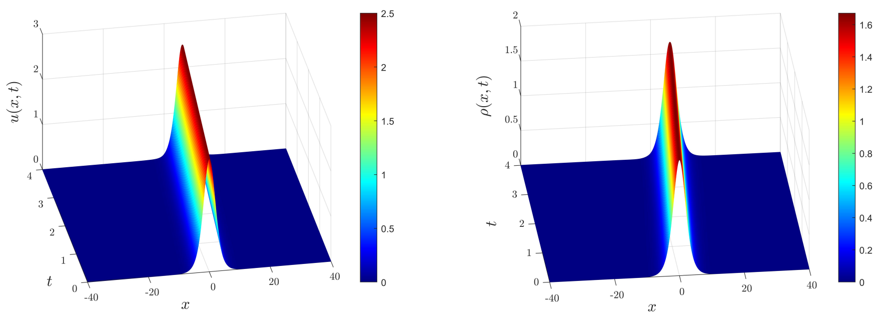

(**a**) (**b**)

Figure 1. Three−dimensional images of $u(x, t)$ (**a**) and $\rho(x, t)$ (**b**) with $h = 1/8, \tau_F = 1/64$.

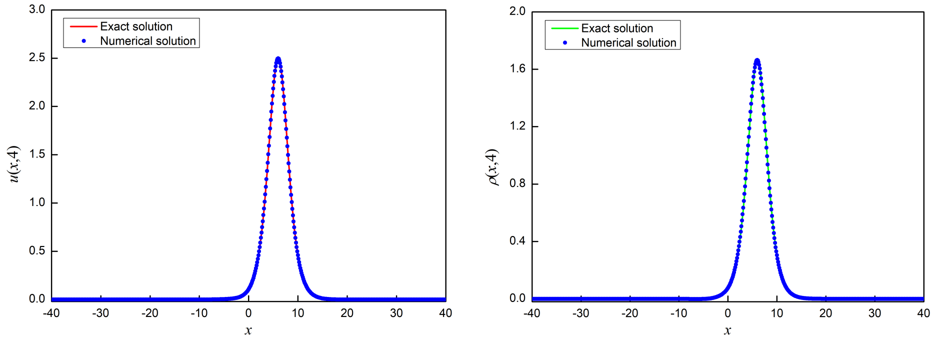

Figure 2. Exact and numerical solution of $u(x,t)$ (**a**) and $\rho(x,t)$ (**b**) at $t = 4$ with $h = 1/8, \tau_F = 1/64$.

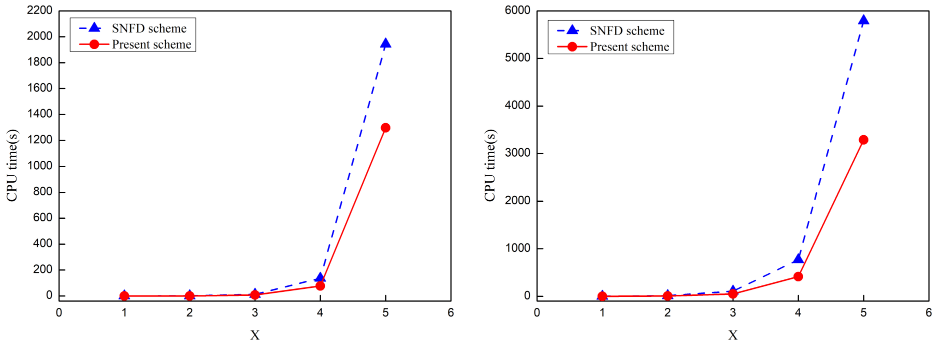

Figure 3. Comparison of CPU times with $\tau_F = h^2$ (**a**) and $h = \tau_F$ (**b**) based on the data in Tables 1 and 2.

5.2. Conservative Approximations

To further verify the accuracy of the new scheme, we calculate four conservation laws of the SRLW Equation (1), such as:

$$Q_1 = \frac{1}{2}\int_{-\infty}^{\infty} \rho dx, \qquad Q_2 = \frac{1}{2}\int_{-\infty}^{\infty} u dx,$$
$$Q_3 = \frac{1}{2}\int_{-\infty}^{\infty} (u^2 + u_x^2 + \rho^2) dx, \quad Q_4 = \frac{1}{2}\int_{-\infty}^{\infty} (\rho u + \frac{1}{6}u^3) dx.$$

Afterwards, employing discrete forms, we are able to compute four approximate conservative quantities which can be represented as

$$Q_1 = \frac{h}{2}\sum_{j=0}^{J-1} \rho_j^n,$$
$$Q_2 = \frac{h}{2}\sum_{j=0}^{J-1} u_j^n,$$
$$Q_3 = \frac{h}{2}\sum_{j=0}^{J-1} (u_j^n)^2 + \frac{1}{2h}\sum_{j=0}^{J-1} (u_{j+1}^n - u_j^n)^2 + \frac{h}{2}\sum_{j=0}^{J-1} (\rho_j^n)^2,$$
$$Q_4 = \frac{h}{2}\sum_{j=0}^{J-1} \rho_j^n u_j^n + \frac{h}{12}\sum_{j=0}^{J-1} (u_j^n)^3.$$

The values of four quantities are recorded in Tables 3–6. In Tables 3 and 4, regardless of the time step and grid spacing, the quantities Q_1 and Q_2 remain well-preserved at various times. In Table 5, for the case $h = 1/2$ and $\tau_F = 1/4$, one can see that the quantity Q_3 experiences a slight increase as time increases, however, as the spatial and temporal step sizes decrease, the variation of Q_3 becomes extremely small. In Table 6, it has been found that for quantity Q_4, there was a minor decline under different mesh steps, but it gradually rebounded over time. Meanwhile, as the spatial and temporal step sizes decrease, the Q_4 increases slightly. Figure 4 plots the variation curves of four quantities for the case $h = 1/8$ and $\tau_F = 1/64$, which visually demonstrate that our scheme preserves the four conservation laws.

Table 3. Quantity Q_1 under different mesh steps h and τ_F at various times.

TT-M Finite Difference Scheme				
	$(\frac{1}{2}, \frac{1}{4})$	$(\frac{1}{4}, \frac{1}{16})$	$(\frac{1}{8}, \frac{1}{64})$	$(\frac{1}{16}, \frac{1}{256})$
$t = 0.0$	4.4721359549	4.4721359549	4.4721359549	4.4721359549
$t = 0.5$	4.4721359549	4.4721359549	4.4721359549	4.4721359549
$t = 1.0$	4.4721359549	4.4721359549	4.4721359549	4.4721359549
$t = 1.5$	4.4721359549	4.4721359549	4.4721359549	4.4721359549
$t = 2.0$	4.4721359549	4.4721359549	4.4721359549	4.4721359549
$t = 2.5$	4.4721359549	4.4721359549	4.4721359549	4.4721359549
$t = 3.0$	4.4721359549	4.4721359549	4.4721359549	4.4721359549
$t = 3.5$	4.4721359549	4.4721359549	4.4721359549	4.4721359549
$t = 4.0$	4.4721359549	4.4721359549	4.4721359549	4.4721359549

Table 4. Quantity Q_2 under different mesh steps h and τ_F at various times.

TT-M Finite Difference Scheme				
	$(\frac{1}{2}, \frac{1}{4})$	$(\frac{1}{4}, \frac{1}{16})$	$(\frac{1}{8}, \frac{1}{64})$	$(\frac{1}{16}, \frac{1}{256})$
$t = 0.0$	6.7082039324	6.7082039324	6.7082039324	6.7082039324
$t = 0.5$	6.7082039324	6.7082039324	6.7082039324	6.7082039324
$t = 1.0$	6.7082039324	6.7082039324	6.7082039324	6.7082039324
$t = 1.5$	6.7082039324	6.7082039324	6.7082039324	6.7082039324
$t = 2.0$	6.7082039324	6.7082039324	6.7082039324	6.7082039324
$t = 2.5$	6.7082039324	6.7082039324	6.7082039324	6.7082039324
$t = 3.0$	6.7082039324	6.7082039324	6.7082039324	6.7082039324
$t = 3.5$	6.7082039324	6.7082039324	6.7082039324	6.7082039324
$t = 4.0$	6.7082039323	6.7082039323	6.7082039323	6.7082039323

Table 5. Quantity Q_3 under different mesh steps h and τ_F at various times.

TT-M Finite Difference Scheme				
	$(\frac{1}{2}, \frac{1}{4})$	$(\frac{1}{4}, \frac{1}{16})$	$(\frac{1}{8}, \frac{1}{64})$	$(\frac{1}{16}, \frac{1}{256})$
$t = 0.0$	17.3814360100	17.3890764778	17.3909982095	17.3914793723
$t = 0.5$	17.3879364459	17.3894925427	17.3910247524	17.3914810404
$t = 1.0$	17.4021575260	17.3904434452	17.3910850544	17.3914848239
$t = 1.5$	17.4178948195	17.3914089843	17.3911453660	17.3914885933
$t = 2.0$	17.4279575149	17.3919924045	17.3911803618	17.3914907570
$t = 2.5$	17.4320624736	17.3921089940	17.3911854445	17.3914910387
$t = 3.0$	17.4298852213	17.3919072419	17.3911710024	17.3914901056
$t = 3.5$	17.4257242289	17.3915916231	17.3911504036	17.3914888028
$t = 4.0$	17.4208004460	17.3913048704	17.3911324701	17.3914876800

Table 6. Quantity Q_4 under different mesh steps h and τ_F at various times.

TT-M Finite Difference Scheme				
	$(\frac{1}{2}, \frac{1}{4})$	$(\frac{1}{4}, \frac{1}{16})$	$(\frac{1}{8}, \frac{1}{64})$	$(\frac{1}{16}, \frac{1}{256})$
$t = 0.0$	29.8645685095	29.8270800111	29.8174683777	29.8150480627
$t = 0.5$	29.5194998279	29.7377964805	29.7949677954	29.8094115019
$t = 1.0$	29.2953094352	29.6804305056	29.7805099425	29.8057894879
$t = 1.5$	29.2373157339	29.6665651150	29.7770997278	29.8049405034
$t = 2.0$	29.3052034101	29.6864373371	29.7822468973	29.8062391542
$t = 2.5$	29.4333002603	29.7204018949	29.7909264484	29.8084218678
$t = 3.0$	29.5520897511	29.7519209103	29.7989376025	29.8104338587
$t = 3.5$	29.6355327196	29.7733189521	29.8043614200	29.8117950932
$t = 4.0$	29.6765644108	29.7843463859	29.8071613054	29.8124980105

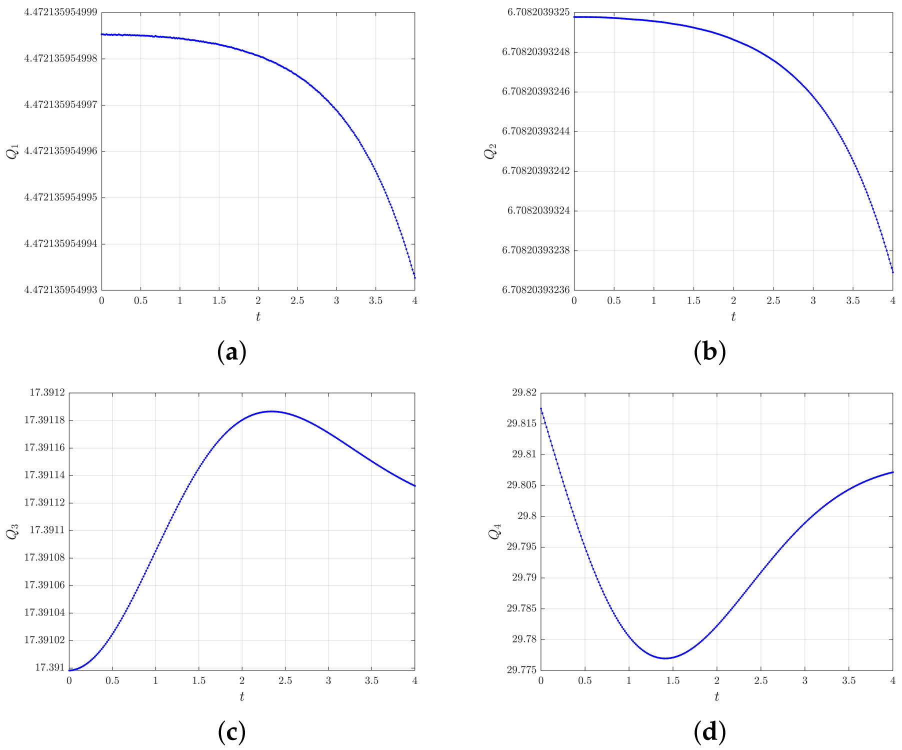

Figure 4. Quantities Q_1 (**a**), Q_2 (**b**), Q_3 (**c**) and Q_4 (**d**) under mesh steps $h = 1/8$, $\tau_F = 1/64$.

5.3. Long-Time Simulation

Using the parameters $h = 0.1$, $\tau_F = 0.01$, $x_L = -20$, $x_R = 100$ and $T = 40$, the long time waveforms of $u(x,t)$ and $\rho(x,t)$ generated by the present scheme are illustrated in Figure 5. The waveforms at t = 20 and 40 demonstrate a significant level of agreement with the waveforms at t = 0, which also indicates the accuracy of the scheme. Figure 6 displays the computational times of both the SNFD scheme and proposed scheme at long time. From the graph, it can be seen that the computational time difference between the two schemes grows increasingly as the simulation time increases, which indicates that the longer the simulation time, the more computational time can be saved by the scheme proposed in this paper. This once again proves the advantage of our scheme compared to the SNFD scheme in [22].

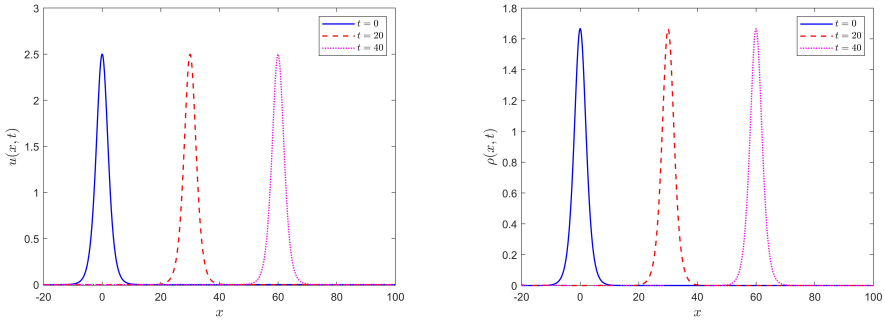

(**a**) (**b**)

Figure 5. Numerical solutions of $u(x,t)$ (**a**) and $\rho(x,t)$ (**b**) at long time with $h = 1/10, \tau_F = 1/100$.

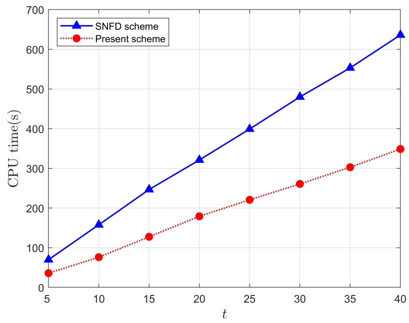

Figure 6. Comparison of computation times of the SNFD scheme in [22] with present scheme at long time under $h = 1/10, \tau_F = 1/100$.

6. Conclusions

This paper presents a new time two-mesh finite difference scheme for solving the symmetric regularized long wave equation, which contains a nonlinear derivative term in its formulation. Based on the previous work, our aim is to obtain a scheme that is not only error-preserving but also can save more computational time compared to the scheme in [22]. To achieve this goal, we have constructed a TT-M finite difference scheme that mainly consists of three steps. Firstly, the time interval is divided into coarse and fine time meshes, then the nonlinear system is solved on the coarse time mesh; secondly, coarse numerical solutions on the fine time mesh are computed using an interpolation formula based on the solutions derived in the step one; lastly, the nonlinear term of the SRLW equation is linearized using Taylor's formula for a function with three variables and constructed the TT-M finite difference linear numerical scheme on the fine time mesh. In terms of theoretical results, we investigated the convergence and stability of numerical solutions. We observed that the solutions obtained from our proposed scheme converged to the exact solutions of the SRLW equation, and the rate of convergence is $O(\tau_C^2 + \tau_F + h^2)$. Additionally, τ_F and h are sufficiently small, then the proposed scheme (8)–(9) is stable with respect to the initial conditions on the fine time mesh. The numerical results demonstrated that the proposed method effectively supported the analysis of the convergence rate. Meanwhile, one can observe that the errors of $u(x,t)$ and $\rho(x,t)$ in both the SNFD scheme in [22] and the present scheme are nearly identical, but the proposed scheme can reduce the computational time compared with the SNFD scheme. In addition, we calculated four conservation laws of the SRLW equation, regardless of the time step and grid spacing; the four quantities remain well-preserved at various times. The long time simulation example of the proposed scheme is also conducted in this part, the result shows that the waveform always maintains its original state in a long time. The error increases gently as simulation time is extended, which is a limitation of the proposed scheme and it will be improved by other methods in our future work. These findings demonstrate that the proposed method is more effective and yields a better improvement in solving the SRLW equation.

Author Contributions: Conceptualization, J.G.; methodology, J.G.; software, J.G. and S.H.; validation, S.H., Q.B. and J.L.; formal analysis, J.G. and S.H.; writing—original draft preparation, J.G.; writing—review and editing, J.G. and S.H.; funding acquisition, S.H., Q.B and J.L. All authors have read and agreed to the published version of the manuscript.

Funding: This work is supported by National Natural Science Foundation of China (Nos. 12161034 and 11961022), Natural Science Foundation of Inner Mongolia (No. 2021MS01017), Natural Scientific Research Innovation Team of Hohhot Minzu College (No. HMTD202005).

Institutional Review Board Statement: Not applicable.

Informed Consent Statement: Not applicable.

Data Availability Statement: All the data were computed using our method.

Acknowledgments: We are grateful to the anonymous reviewers for their valuable suggestions and comments.

Conflicts of Interest: The author declare no conflict of interest.

References

1. Peregrine, D.H. Calculations of the development of an undular bore. *J. Fluid Mech.* **1966**, *25*, 321–330. [CrossRef]
2. Peregrine, D.H. Long waves on beach. *J. Fluid Mech.* **1967**, *27*, 815–827. [CrossRef]
3. Korteweg, D.J.; de Vries, G. On the change of form of long waves advancing in a rectangular canal, and on a new type of long stationary waves. *Philos. Mag.* **1895**, *39*, 422–443. [CrossRef]
4. Seyler, C.E.; Fenstermacher, D.L. A symmetric regularized-long-wave equation. *Phys. Fluids* **1984**, *27*, 4–7. [CrossRef]
5. Fang, S.; Guo, B.; Qiu, H. The existence of global attractors for a system of multi-dimensional symmetric regularized wave equations. *Commun. Nonlinear Sci. Numer. Simul.* **2009**, *14*, 61–68.
6. Xu, F. Application of Exp-function method to symmetric regularized long wave (SRLW) equation. *Phys. Lett. A* **2008**, *372*, 252–257. [CrossRef]
7. Abazari, R. Application of (G'/G)-expansion method to travelling wave solutions of three nonlinear evolution equation. *Comput. Fluids* **2010**, *39*, 1957–1963. [CrossRef]
8. Chand, F.; Malik, A.K. Exact traveling wave solutions of some nonlinear equations using(G'/G)-expansion method. *Int. J. Nonlinear Sci.* **2012**, *14*, 416–424.
9. Yalçınkaya, İ.; Ahmad, H.; Tasbozan, O.; Kurt, A. Soliton solutions for time fractional ocean engineering models with Beta derivative. *J. Ocean Eng. Sci.* **2022**, *7*, 444–448. [CrossRef]
10. Mamun, A.A.; Ananna, S.N.; An, T.; Shahen, N.H.M.; Asaduzzaman, M. Dynamical behaviour of travelling wave solutions to the conformable time-fractional modified Liouville and mRLW equations in water wave mechanics. *Heliyon* **2021**, *7*, e07704. [CrossRef]
11. Hussain, A.; Jhangeer, A.; Abbas, N.; Khan, I.; Nisar, K.S. Solitary wave patterns and conservation laws of fourth-order nonlinear symmetric regularized long-wave equation arising in plasma. *Ain Shams Eng. J.* **2021**, *12*, 3919–3930. [CrossRef]
12. Lu, D.; Seadawy, A.R.; Ali, A. Applications of exact traveling wave solutions of modified Liouville and the symmetric regularized long wave equations via two new techniques. *Results Phys.* **2018**, *9*, 1403–1410. [CrossRef]
13. Manafian, J.; Zamanpour, I. Exact travelling wave solutions of the symmetric regularized long wave (SRLW) using analytical methods. *Stat. Optim. Inf. Comput.* **2014**, *2014*, 47–55.
14. Sendi, C.T.; Manafian, J.; Mobasseri, H.; Mirzazadeh, M.; Zhou, Q.; Bekir, A. Application of the ITEM for solving three nonlinear evolution equations arising in fluid mechanics. *Nonlinear Dyn.* **2019**, *95*, 669–684. [CrossRef]
15. Bekir, A. New solitons and periodic wave solutions for some nonlinear physical models by using the sine–cosine method. *Phys. Scr.* **2008**, *77*, 045008. [CrossRef]
16. Guo, B. The spectral method for symmetric regularized wave equations. *J. Comput. Math.* **1987**, *5*, 297–306.
17. Zheng, J.; Zhang, R.; Guo, B. The Fourier pseudo-spectral method for the SRLW equation. *Appl. Math. Mech.* **1989**, *10*, 801–810.
18. Wang, T.C.; Zhang, L.M.; Chen, F.Q. Conservative schemes for the symmetric regularized long wave equations. *Appl. Math. Comput.* **2007**, *190*, 1063–1080. [CrossRef]
19. Yimnet, S.; Wongsaijai, B.; Rojsiraphisal, T.; Poochinapan, K. Numerical implementation for solving the symmetric regularized long wave equation. *Appl. Math. Comput.* **2016**, *273*, 809–825. [CrossRef]
20. Hu, J.S.; Zheng, K.L.; Zheng, M.B. Numerical simulation and convergence analysis of high-order conservative difference scheme for SRLW equation. *Appl. Math. Model.* **2014**, *38*, 5573–5581. [CrossRef]
21. Li, S.G. Numerical study of a conservative weighted compact difference scheme for the symmetric regularized long wave equations. *Numer. Methods Partial. Differ. Equ.* **2019**, *35*, 60–83. [CrossRef]
22. Bai, Y.; Zhang, L.M. A conservative finite difference scheme for symmetric regularized long wave equations. *Acta Math. Appl. Sin.* **2007**, *30*, 248–255.

23. Xu, Y.C.; Hu, B.; Xie, X.P.; Hu, J.S. Mixed finite element analysis for dissipative SRLW equations with damping term. *Phys. Fluids* **2012**, *218*, 4788–4797. [CrossRef]
24. He, Y.Y.; Wang, X.F.; Cheng, H.; Deng, Y.Q. Numerical analysis of a high-order accurate compact finite difference scheme for the SRLW equation. *Appl. Math. Comput.* **2022**, *418*, 126837. [CrossRef]
25. Liu, Y.; Yu, Z.D.; Li, H.; Liu, F.W.; Wang, J.F. Time two-mesh algorithm combined with finite element method for time fractional water wave model. *Int. J. Heat Mass Transf.* **2018**, *120*, 1132–1145. [CrossRef]
26. Yin, B.L.; Liu, Y.; Li, H.; He, S. Fast algorithm based on TT-M FE system for space fractional Allen-Cahn equations with smooth and non-smooth solutions. *J. Comput. Phys.* **2019**, *379*, 351–372. [CrossRef]
27. Liu, Y.; Fan, E.Y.; Yin, B.L.; Li, H.; Wang, J.F. TT-M finite element algorithm for a two-dimensional space fractional Gray-Scott model. *Comput. Math. Appl.* **2020**, *80*, 1793–1809. [CrossRef]
28. Wen, C.; Liu, Y.; Yin, B.L.; Li, H.; Wang, J.F. Fast second-order time two-mesh mixed finite element method for a nonlinear distributed-order sub-diffusion model. *Numer. Algorithms* **2021**, *88*, 523–553. [CrossRef]
29. Tian, J.L.; Sun, Z.Y.; Liu, Y.; Li, H. TT-M Finite Element Algorithm for the Coupled Schrödinger–Boussinesq Equations. *Axioms* **2022**, *11*, 314. [CrossRef]
30. Qiu, W.L.; Xu, D.; Guo, J.; Zhou, J. A time two-grid algorithm based on finite difference method for the two-dimensional nonlinear time-fractional mobile/immobile transport model. *Numer. Algorithms* **2020**, *85*, 39–58. [CrossRef]
31. Xu, D.; Guo, J.; Qiu, W.L. Time two-grid algorithm based on finite difference method for two-dimensional nonlinear fractional evolution equations. *Appl. Numer. Math.* **2019**, *152*, 169–184. [CrossRef]
32. Niu, Y.X.; Liu, Y.; Li, H.; Liu, F.W. Fast high-order compact difference scheme for the nonlinear distributed-order fractional Sobolev model appearing in porous media. *Math. Comput. Simul.* **2023**, *203*, 387–407. [CrossRef]
33. He, S.; Liu, Y.; Li, H. A time two-mesh compact difference method for the one-dimensional nonlinear schrödinger equation. *Entropy* **2022**, *24*, 806. [CrossRef] [PubMed]
34. Zhou, Y.L. *Application of Discrete Functional Analysis to the Finite Difference Method*; International Academic Publishers: Beijing, China, 1990.